

Article

Effect of Temperature on Corrosion Resistance of Layered Double Hydroxides Conversion Coatings on Magnesium Alloys Based on a Closed-Cycle System

Xiaochen Zhang ¹, Zhijuan Yin ^{1,†}, Bateer Buhe ¹, Jiajie Wang ^{1,*}, Lin Mao ^{2,*}, Bin Liu ³, Peng Zhou ^{4,†}, Yang Zhao ⁴, Tao Zhang ⁴ and Fuhui Wang ⁴

- ¹ Heilongjiang Institute of Technology, College of Materials Chemical and Engineering, Harbin 150050, China; zxc2013@hrbeu.edu.cn (X.Z.); xiaojuan8065@126.com (Z.Y.); bate1976@sina.com (B.B.)
- ² School of Medical Instrument and Food Engineering, University of Shanghai for Science and Technology, Shanghai 200093, China
- ³ College of Materials Science and Chemical Engineering, Harbin Engineering University, Harbin 150001, China; liubin@hrbeu.edu.cn
- ⁴ Shenyang National Laboratory for Materials Science, Corrosion and Protection Division, Northeastern University, Shenyang 110819, China; zhoupeng@mail.neu.edu.cn (P.Z.); zhaoyang7402@mail.neu.edu.cn (Y.Z.); zhangtao@mail.neu.edu.cn (T.Z.); fhwang@mail.neu.edu.cn (F.W.)
- * Correspondence: wangjiajie2006@126.com (J.W.); linmao@usst.edu.cn (L.M.)
- † Contributing equally.



Citation: Zhang, X.; Yin, Z.; Buhe, B.; Wang, J.; Mao, L.; Liu, B.; Zhou, P.; Zhao, Y.; Zhang, T.; Wang, F. Effect of Temperature on Corrosion Resistance of Layered Double Hydroxides Conversion Coatings on Magnesium Alloys Based on a Closed-Cycle System. *Metals* **2021**, *11*, 1658. <https://doi.org/10.3390/met11101658>

Academic Editors: Sebastian Feliú, Jr. and David M. Bastidas

Received: 1 September 2021
Accepted: 14 October 2021
Published: 19 October 2021

Publisher's Note: MDPI stays neutral with regard to jurisdictional claims in published maps and institutional affiliations.



Copyright: © 2021 by the authors. Licensee MDPI, Basel, Switzerland. This article is an open access article distributed under the terms and conditions of the Creative Commons Attribution (CC BY) license (<https://creativecommons.org/licenses/by/4.0/>).

Abstract: The effect of temperature on the corrosion resistance of layered double hydroxide (LDH) conversion coatings on AZ91D magnesium alloy, based on a closed-cycle system, was investigated. Scanning electron microscopy (SEM), photoelectron spectroscopy (XPS), and X-ray diffractometry (GAXRD) were used to study the surface morphology, chemical composition, and phase composition of the conversion coating. The corrosion resistance of the LDH conversion coating was determined through electrochemical polarization curve and hydrogen evolution and immersion tests. The results showed that the conversion coating has the highest density and a more uniform, complete, and effective corrosion resistance at 50 °C. The chemical composition of the LDH conversion coating mainly comprises C, O, Mg, and Al, and the main phase is $Mg_6Al_2(OH)_{16}CO_3 \cdot 4H_2O$.

Keywords: AZ91D magnesium alloy; LDH conversion coating; closed-cycle system; temperature; corrosion resistance

1. Introduction

Magnesium alloys have been believed to be “the green engineering material of the 21st century”, and have met wide application prospects in automotive, aerospace, electronics, and biomedical fields [1,2]. Especially with the development of magnesium alloy processing or preparation technology and maturity, including already preparing micro/nanoscale magnesium alloy materials, this gives the development of magnesium alloys a more prominent advantage [3–9]. However, the poor corrosion resistance of magnesium alloys is still an unsolved scientific issue [10,11].

Surface treatment has been, so far, one of the most effective and convenient ways of improving the corrosion resistance of magnesium alloys [12–14]. The porous oxide/hydroxide coatings formed on the surface of magnesium alloys are not able to protect anti-corrosion. The galvanic corrosion tends to be formed for the potential difference of the second phase, impurity phase and base phase [15–17]. In addition, stress corrosion or fatigue, which is caused by residual internal stress, can accelerate the corrosion of magnesium alloys [18–20]. Protective coatings of magnesium alloys can isolate magnesium alloy from the corrosive medium, thereby conferring a better protection. Common surface treatments of magnesium alloys include micro-arc/anodizing, electroplating/electroless plating, laser surface

treatment, chemical conversion treatment, organic coating treatment, surface infiltration treatment, and ion implantation [21–26]. Among all surface treatment methods, chemical conversion treatment has been widely applied due to its low energy consumption, low costs, simple equipment, and easy operation [27,28]. For example, chromate conversion coating, phosphate conversion coating, phosphate–permanganate conversion coating, stannate conversion coating, vanadate conversion coating, cerium conversion coating, and lanthanide conversion coating [29–31]. With the improvement of environmental consciousness, chromate conversion coating has been banned, and low-cost, green, efficient and environmentally friendly conversion coating has become the research target [32,33]. In all the newly developed conversion coating methods, layered double hydroxides have attracted much attention due to their unique intercalation structure and environmental protection properties [34–36]. Layered double hydroxides (LDHs) can be represented by a general formula of $[M_{1-x}^{2+}M_x^{3+}(\text{OH})_2][A^{n-}]_{x/n} \cdot m\text{H}_2\text{O}$, where M^{2+} and M^{3+} represent divalent (e.g., Mg^{2+} , Ca^{2+} , Cu^{2+} , Mn^{2+} , Ni^{2+} , Zn^{2+}) and trivalent metallic cations (e.g., Al^{3+} , Cr^{3+} , Fe^{3+} , Mn^{3+} , Co^{3+}), respectively. X indicates the molar ratio of $M^{3+}/(M^{2+} + M^{3+})$ and its value ranges from 0.20 to 0.33; finally, A^{n-} is an n^- valent anion, which is an exchangeable anion. The anions (e.g., Cl^- , CO_3^{2-} , NO_3^- , and SO_4^{2-}) and the variety of organic anions can be exchanged between the outside and interlayer spaces occupied by the water molecules [37,38]. Uan et al. [39,40] carried out some research on the hydrotalcite coatings prepared on magnesium alloys by the one-step method. The Mg-Al-hydrotalcite LDH coatings were prepared by the carbonate/bicarbonate solutions stand at 50 °C for 24 h, which was recorded as CO₂_24h [41,42]. Based on the previous research, Uan et al. adopted a two-step method by a 2 h CO₂ and pH 11.5 treatment to modify the chemical technique; this was recorded as CO₂_2h/pH11.5_2h [43–45]. It was found that the formation effect was improved by adjusting the pH value. However, the time was found to be relatively long with a complex treatment. Chen et al. [46,47] studied the preparation of Mg-Al hydrotalcite coatings on AZ31 Mg alloys by the two-step method. It was found that the precursor coating with cracks initially formed; then, LDH conversion coatings formed densely and compactly. Although the processing time was shortened to 2 h, the formation process was relatively complex [48–50]. Zhang et al. [51,52] put forward the ion exchange and corrosion resistance properties by preparing MgAl-LDH coatings on Mg and Al alloys.

The preparation of traditional LDH conversion coatings is almost completely concentrated on the standard atmospheric pressure of the open system, and the conversion coating in the closed-cycle system is rarely involved. The traditional methods in the preparation of LDH conversion coatings have the several shortcomings. On the one hand, they are time-consuming. A long preparation time is not conducive to the batch processing of conversion coating; on the other hand, it is complex. The treatment solution needs to be preprepared for many times and replaced each time, which requires a lot of labour. Therefore, solving the aforementioned issues is the key to improving the research of hydrotalcite coating surface treatment. The author's previous study found that the CO₂ pressurization method can greatly improve the preparation efficiency of conversion coating. The treatment solution can be recycled without affecting the formation effect. So, the author proposed a CO₂ pressurization method for the first time, and the effect of CO₂ pressure and treatment time on the corrosion resistance of LDH conversion coating was studied, and the formation mechanism of the micro-galvanic regions with different β -phase morphology on the magnesium alloy was proposed [53–55]. The author found that temperature is also an important factor under the closed-cycle system, and the microstructures of LDH conversion coatings are quite different at low and high temperatures. Therefore, the main purpose of this paper is to study the effect of temperature on the microstructure and corrosion resistance of LDH conversion coating. The research results of temperature are the perfection of and supplement to CO₂ pressurization technology. At the same time, it provides a reliable theoretical basis for the development of new magnesium alloy conversion coating treatment technologies.

2. Materials and Methods

2.1. Sample Preparation

The experimental materials used in this study are commercial as-cast AZ91D magnesium alloys. Its chemical composition is analysed by ICP-OES (inductively coupled plasma-emission spectrometry). Firstly, we should separately obtain a 0.1 g sample from different parts of sheet metal and place it in nitric acid solution, stirring until completely dissolved. Secondly, we should transfer this solution to a 1 L volumetric flask, dilute it with distilled water to volume, and mix. Finally, we should measure the content by ICP-OES and calculate the mean value. The chemical compositions of the main elements: 8.8 wt.% Al, 0.69 wt.% Zn, 0.212 wt.% Mn, 0.02 wt.% Si, 0.002 wt.% Cu, 0.005 wt.% Fe, and 0.001 wt.% Ni. The ingot was cut into sizes 20 mm × 20 mm × 6 mm by wire cutting, and a round hole of 2 mm was made at the top for hanging the samples. The samples were polished using SiC abrasive papers of 1000#–2000# mesh. The samples were washed with distilled water and then cleaned ultrasonically with anhydrous ethanol for 15 min. The samples were dried in cold air for reserve use.

2.2. CO₂ Pressurisation Method Preparation Process

The CO₂ pressurisation method is a closed-cycle preparation method of AZ91D magnesium alloy LDH conversion coating. It is based on the formation process of LDH conversion on magnesium alloys and on the characteristics of CO₃²⁻/HCO₃⁻ ion formation solution [39,40]. The aim was to increase the reaction rate and stability of the formation system by applying CO₂ partial pressure to the formation system and prepare an LDH conversion coating in the shortest possible time frame, incurring the lowest cost. The method followed was that, at room temperature, industrial CO₂ was continuously passed into 1000 mL of deionised water to prepare the conversion solution, in which CO₂ gas was passed at a rate of 1 dm³·min⁻¹. The time elapsed was 20 min, and the pH of the solution was ~4.3. The conversion coating solution and the treated samples were then placed into a closed coating making chamber. The pressure of the coating was controlled at 3 MPa by CO₂ pressurisation. The time taken for successful conversion was 30 min, and the successive temperatures of the coating were set as 30 °C, 40 °C, 50 °C, 60 °C, and 80 °C, shown in Figure 1.

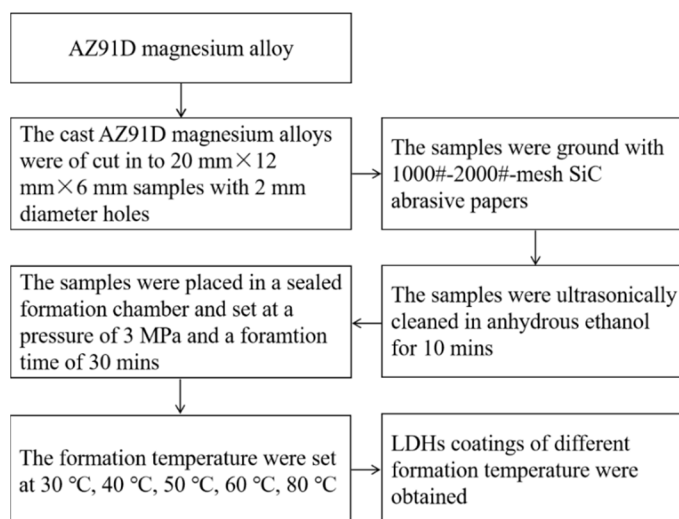


Figure 1. Operations for the preparation of conversion coating with CO₂ pressurisation method.

2.3. Test Methods

The surface and cross-sectional morphologies of LDH coatings were observed using a Philips XL30 (PHILIPS Inc., Amsterdam, NL) and a JEOL JSM-6700F SEM (JEOL Inc., Akishima-shi, TKY, Japan), respectively. The elemental composition of the conversion

coating was analysed using a K-Alpha XPS X-ray energy spectrometer. A monochromatic Al target was used. The Al $K\alpha h\nu = 1486.6$ eV sample analysis area was $700 \mu\text{m} \times 300 \mu\text{m}$ (inorganic material), less than 5 nm (organic material), and less than 5 nm (X-ray working power, generally 150 W). The phase composition of the chemical conversion coating was analysed through X-ray diffraction (Cu target, $\lambda = 0.154059$ nm, 30 mA, 40 kV) with a scanning range of $5\text{--}55^\circ$ and a step length of 0.02° , scattering angle 0.4° .

The potentiodynamic polarisation measurements of the samples were taken in an electrochemical workstation (Zahner Zennium)(ZAHNER Inc., Kronach, Germany), with a three-electrode cell, using a platinum foil as the counter electrode and a saturated calomel electrode (SHE) (saturated KCl) as the reference electrode in an aerated 3.5 wt.% NaCl solution. The corrosion of the magnesium alloy was represented by the hydrogen evolution of the cathode. To avoid the influence of the cathode process on the whole electrochemical testing process, the anodic and cathodic polarisation curves of the specimens were measured from the open circuit potential to the anodic and cathodic sides in the 300 mV range, with a scan rate of $0.333 \text{ mV}\cdot\text{s}^{-1}$, respectively. All the above measurements were repeated at least five times. The hydrogen evolution data were measured by collecting hydrogen from the reaction in a hydrogen collector. The samples were placed in a beaker containing 3.5 wt.% NaCl solution and a water bath pot maintained at a constant temperature of 30 ± 1 °C. The burette was connected to the funnel and was inverted into the solution (perpendicular to the sample being tested). The top of the burette was fully immersed in the solution. The hydrogen bubbles produced as a result of magnesium alloy corrosion was introduced into the burette through the funnel so that the hydrogen evolution rate of the magnesium alloy and the coating could be determined by the change in readings on the burette after the hydrogen was collected. All of the hydrogen measurements were repeated at least three times. The immersion test was conducted to determine the corrosion rank of the LDH coating samples. For the immersion test, all measurements were repeated at least three times at 30 ± 1 °C. In the immersion test, digital cameras were used to record the macroscopic morphology before and during the corrosion process. Observations were made every 24 h and photos were also captured.

3. Results and Analysis

3.1. Microstructure

The surface and cross-sectional morphologies of the LDH coatings at different formation temperatures are shown in Figures 2 and 3, respectively. It can be seen that the characteristics of the LDH conversion coatings vary greatly at different temperatures in Figure 2. When the temperature is low (at 30 °C), the conversion coating does not have any obvious honeycomb structure characteristics (Figure 2a), while as the temperature increases to 40 °C, the conversion coating gradually exhibits honeycomb characteristics (Figure 2b). It merits our attention that the honeycomb structure is more prominent at 50 °C (Figure 2c,f).

At 60 °C, the honeycomb structure of the LDH conversion coating is very similar to that at 50 °C, but cracks have appeared (Figure 2d). When the temperature is too high (at 80 °C), the honeycomb structure and the uneven structures with cracks alternate (Figure 2e). This is consistent with the test results obtained from the cross-sectional morphology of LDH conversion coating in Figure 3. In Figure 3a, incomplete LDH conversion coating can be observed. The conversion coating of different nucleation sites does not form complete binding, and the existence of cracks can be noticed clearly. With the increase in temperature, the crack in the conversion coating weakens (Figure 3b). At 50 °C, the LDH conversion coating is very uniform and dense (Figure 3c). However, at 60 °C, the initiation site of the cracks is also visible (Figure 3d). At 80 °C, the cracks of the LDH conversion coating become more severe (Figure 3e,f).

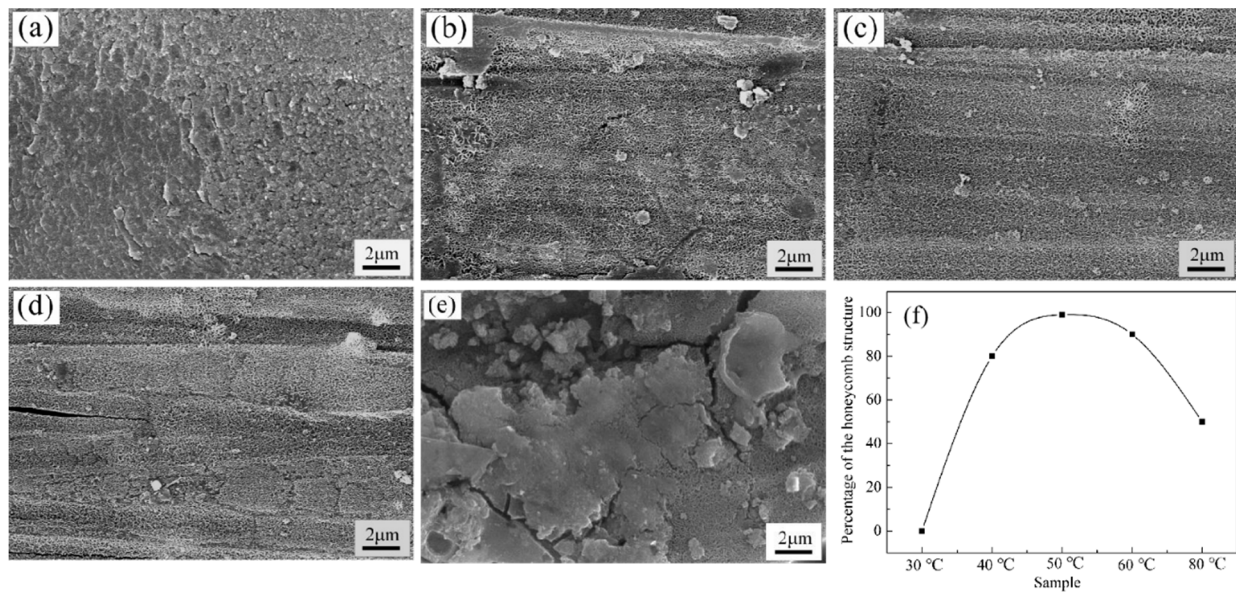


Figure 2. Surface morphology of the layered double hydroxide (LDH) coatings at different temperatures for a closed-cycle system: (a) 30, (b) 40, (c) 50, (d) 60, and (e) 80 °C. (f) Percentage of the honeycomb structure for samples.

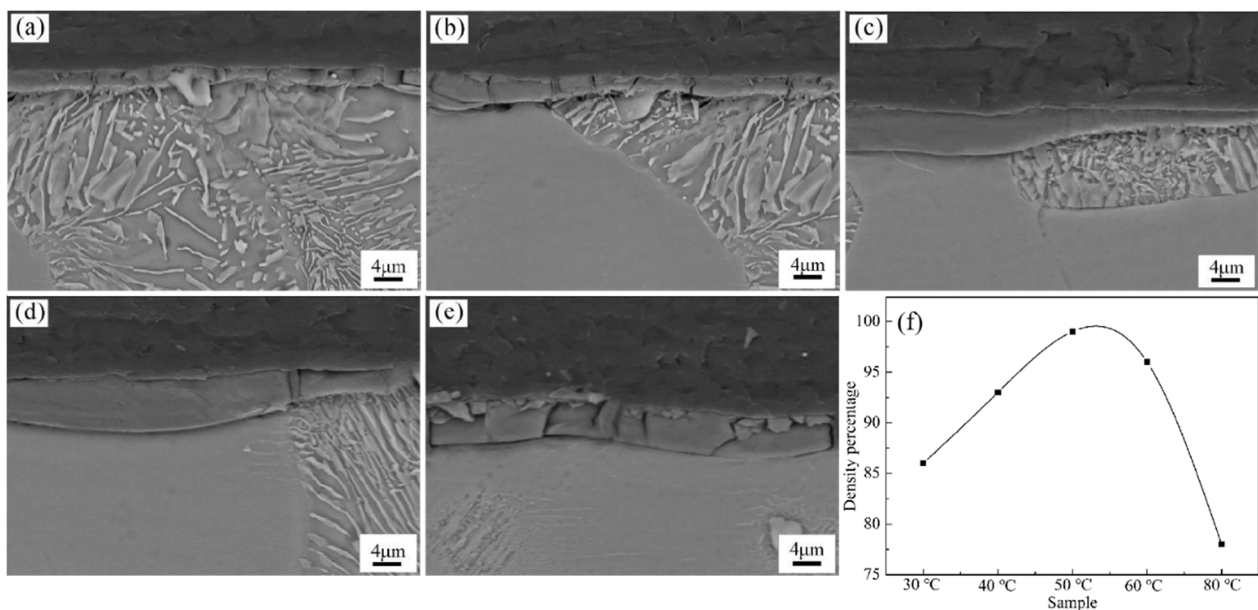


Figure 3. Cross-sectional morphologies of the LDH coatings at different temperatures for a closed-cycle system: (a) 30, (b) 40, (c) 50, (d) 60, and (e) 80 °C. (f) density percentage of the LDH conversion coating samples.

The XPS was employed to investigate the elemental composition and superficial chemical status of the LDH conversion coating. In the XPS survey spectrum of the LDH conversion coating at different temperatures and at of CO₂ 3MPa (Figure 4a), the peaks assigned to Mg 1s, Al 2p, O 1s and C 1s revealed the successful depositing of coating (Figure 4b). From Figure 4, it is found that the main components of the LDH conversion coating on the AZ91D magnesium alloy are O, C, Al, and Mg elements. At 50 °C, Al and Mg begin to participate in the deposition process of conversion coating. This indicates that increasing the temperature promotes the growth of the LDH conversion coating.

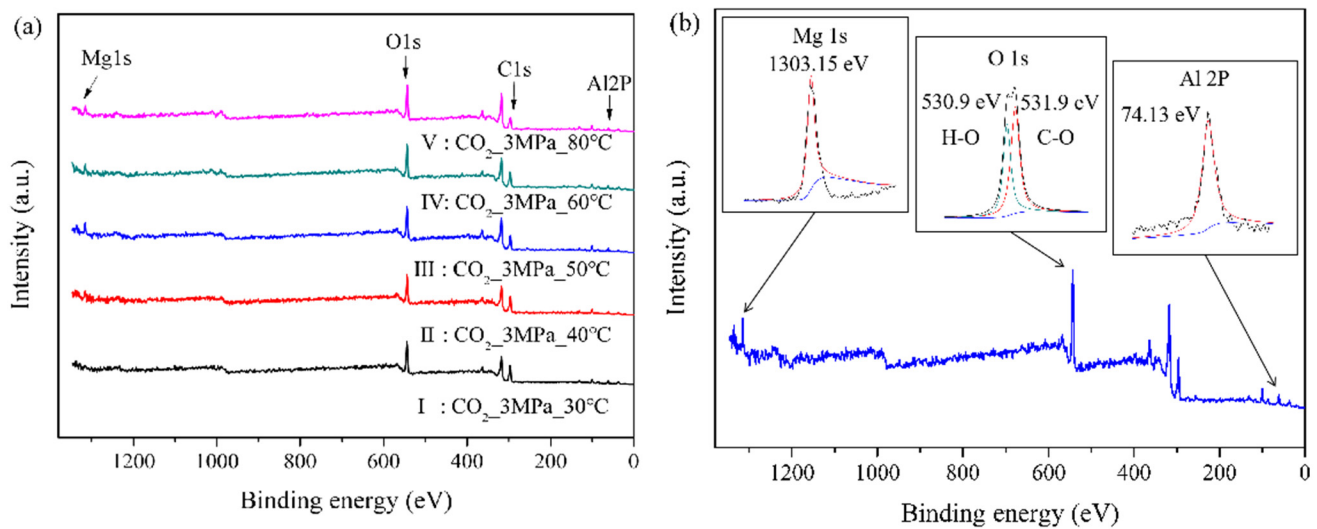


Figure 4. XPS spectra of the LDH conversion coatings at different temperatures at of CO₂ 3MPa: (a) survey spectra, (b) the deconvolution of the CO₂_3MPa_50 °C.

The GAXRD was employed to investigate the crystal structure of the LDH conversion coating at different temperatures and at of CO₂ 3MPa (Figure 5). Figure 5 also reveals that, with an increase in temperature, the crystal structure of Mg₆Al₂(OH)₁₆CO₃·4H₂O becomes more obvious. The characteristic peaks of the LDH conversion coating can be clearly observed at angles of 10.9016°. The 0 0 3 reflection of the LDH phase with a basal spacing of 0.73 nm agrees well with the published values for Mg-Al hydroxalite loads with carbonate anions [42,43]. When the temperature is too low, the conversion coating is just about to form the crystal structure of LDHs but is not complete yet. Crystallisation again deteriorates when the temperature is too high.

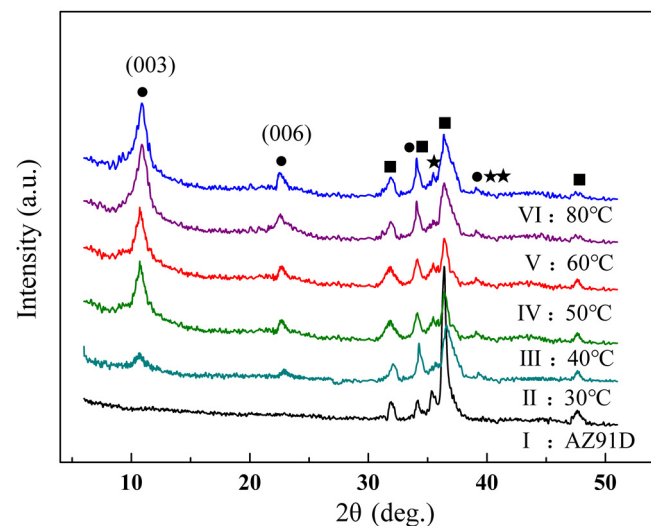


Figure 5. GAXRD patterns of the LDH coatings at different formation temperatures at of CO₂ 3MPa: ★ behalf of the Mg₆Al₂(OH)₁₆CO₃·4H₂O, ■ behalf of the Mg, ● behalf of the Mg₁₇Al₁₂.

3.2. Anti-Corrosion Property

The potentiodynamic polarisation curves (in 3.5 wt.% NaCl solution) of the LDH coatings were tested using the three-electrode system, as indicated in Figure 6. According to the Butler–Volmer equation, the corrosion potential E_{corr} and the corrosion current i_{corr} based on the Tafel extrapolation method were determined. The results are shown in Table 1. The hydrogen evolution data (HER) of the LDH coatings at different formation times in

3.5 wt.% NaCl solution are shown in Figure 7. The immersion test results of 120 h were used to evaluate the corrosion resistance of the LDH coatings (indicated in Figure 8).

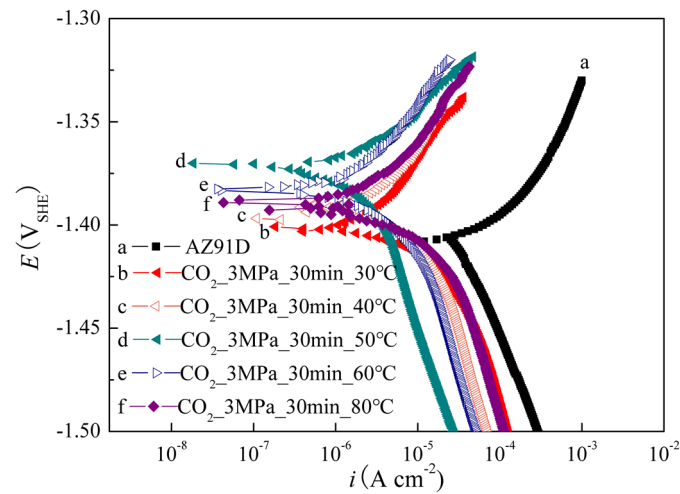


Figure 6. Polarisation curves of the specimens cast, AZ91D magnesium and the LDH conversion coating, with various processes on AZ91D alloy in 3.5 wt.% NaCl solution.

Table 1. Electrochemical test results of the specimens cast, AZ91D magnesium and the layered double hydroxide (LDH) conversion coating, with various processes.

Specimens	Process Parameters	E_{corr} (V vs. SHE)	i_{corr} ($\mu\text{A}\cdot\text{cm}^{-2}$)	Efficiency %
1	AZ91D	$-1.41 (\pm 0.059)$	$83.62 (\pm 1.67)$	-
2	CO_2 _3MPa_30min_30 °C	$-1.40 (\pm 0.054)$	$80.22 (\pm 1.63)$	4.07%
3	CO_2 _3MPa_30min_40 °C	$-1.38 (\pm 0.029)$	$40.64 (\pm 1.63)$	51.40%
4	CO_2 _3MPa_30min_50 °C	$-1.36 (\pm 0.034)$	$8.92 (\pm 1.63)$	89.33%
5	CO_2 _3MPa_30min_60 °C	$-1.37 (\pm 0.053)$	$20.76 (\pm 1.63)$	75.17%
6	CO_2 _3MPa_30min_80 °C	$-1.39 (\pm 0.057)$	$48.53 (\pm 1.63)$	41.96%

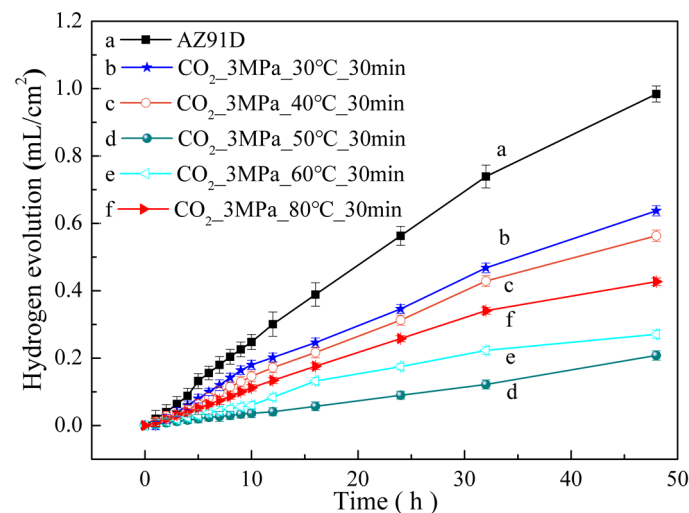


Figure 7. Hydrogen evolution curve of the specimens cast, AZ91D magnesium and the LDH conversion coating, with various processes on AZ91D alloy in 3.5 wt.% NaCl solution.

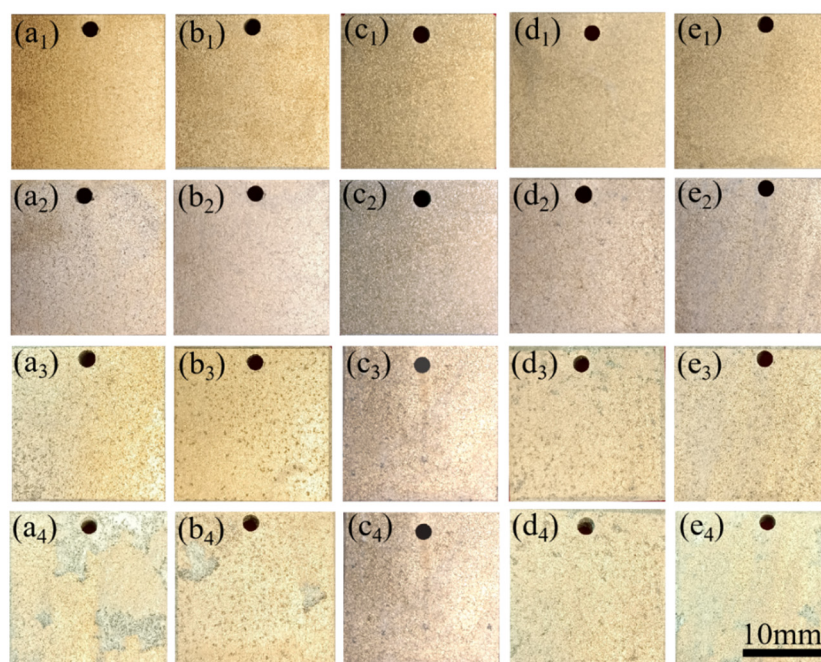


Figure 8. Optical corrosion morphologies of the LDH coatings at different formation times after 120 h of immersion in a 3.5 wt.% NaCl solution. In the above Figure, (a₁) corresponds to the sample at 30 °C immersed for 0 h, (a₂) 30 °C sample immersed for 24 h, (a₃) 30 °C sample immersed for 48 h (a₄) 30 °C sample immersed for 72 h, (b₁) 40 °C sample immersed for 0 h, (b₂) 40 °C sample immersed for 24 h, (b₃) 40 °C sample immersed for 48 h, (b₄) 40 °C sample immersed for 72 h, (c₁) 50 °C sample immersed for 0 h, (c₂) 50 °C sample immersed for 24 h, (c₃) 50 °C sample immersed for 48 h, (c₄) 50 °C sample immersed for 72 h, (d₁) 60 °C sample immersed for 0 h, (d₂) 60 °C sample immersed for 24 h, (d₃) 60 °C sample immersed for 48 h, (d₄) 60 °C sample immersed for 72 h, (e₁) 80 °C sample immersed for 0 h, (e₂) 80 °C sample immersed for 24 h, (e₃) 80 °C sample immersed for 48 h, and (e₄) 80 °C sample immersed for 72 h.

From the sample electrochemical test results, the E_{corr} ($1.36\text{V} \pm 0.034$) of the LDH conversion coating at 50 °C was higher than that of the AZ91D magnesium alloy ($-1.41\text{V} \pm 0.059$) and tends to be more positive at 50 °C. The i_{corr} ($8.92 \pm 1.37 \mu\text{A}\cdot\text{cm}^{-2}$) of the LDHs conversion coating prepared at 50 °C was nearly one order of magnitude lower than that of the AZ91D magnesium alloy ($83.62 \pm 1.63 \mu\text{A}\cdot\text{cm}^{-2}$). The E_{corr} and i_{corr} of samples with LDH conversion coating have a certain error but agree well with the published values [53–55]. The results indicate that the LDH conversion coating prepared at 50 °C can effectively enhance the corrosion resistance of the AZ91D magnesium alloy matrix. In addition, the percentage of efficiency calculated by i_{corr} also shows that the LDH conversion coating prepared at 50 °C has the highest corrosion efficiency.

From the hydrogen evolution test results in 3.5 wt.% NaCl solution (Figure 7), it can be observed that, at the initial stage of the test, the hydrogen evolution rate of the LDH conversion coating prepared at different temperatures was similar. However, with the extension of soaking time, the hydrogen evolution rate of the LDH conversion coating showed a great difference. The HER value of CO₂_3MPa_30min_50 °C sample ($0.624 \pm 0.028 \text{ mL}\cdot\text{h}^{-1}\cdot\text{cm}^{-2}$) was nearly three times lower than that of the AZ91D magnesium alloy ($1.920 \pm 0.114 \text{ mL}\cdot\text{h}^{-1}\cdot\text{cm}^{-2}$), which suggests that the corrosion resistance of the AZ91D alloy can be effectively improved by the conversion coating prepared at 50 °C.

Based on the macro corrosion morphology (Figure 8), it can be observed that, after continuous immersion in 3.5 wt.% NaCl solution for 72 h, the corrosion resistance of the LDH conversion coating prepared at different temperatures was effective in the short immersion test. However, with an increase in immersion test time, the pitting corrosion damage of the

LDH conversion coating began to appear in the NaCl solution. The corrosion behaviour exhibited by the LDH conversion coating, prepared at different temperatures, varied.

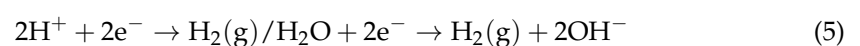
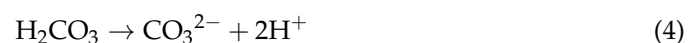
The patterns of LDH conversion coatings indicate that serious pitting corrosion occurs at lower temperatures of 30 °C and 40 °C and higher temperatures of 80 °C when immersed in 3.5 wt.% NaCl solution for 48h; however, the LDH conversion coatings at 50 °C remained intact, and only slight corrosion points were noticed at 60 °C. According to the ASTM (American Society of Testing Materials) D610-08, after soaking for 72 h, the LDH conversion coating samples' corrosion grades were 3G, 3G, and 3G for the samples at 30 °C, 40 °C, 80 °C, respectively. The corrosion grade at 50 °C was 7G and at 60 °C was 6G. From the immersion test results, it can be ascertained that LDH conversion coating can effectively improve the corrosion resistance of the magnesium alloy, wherein LDH conversion coating carried out at 50 °C renders a better protective effect on the surface of the magnesium alloy.

The corrosion resistance is closely related to the microstructure of the LDH conversion coating. At 50 °C, the LDH conversion coating shows the highest density, as well as more uniform and complete morphology in Figures 2c and 3c. Therefore, the LDH conversion coating exhibits the best corrosion resistance at 50 °C. In contrast, as the temperatures become higher or lower, the conversion coating is either incompletely formed or cracked during deposition. The LDH conversion coating with incomplete growth, cracks and insufficient density cannot provide effective protection for the magnesium alloy. By a long-term immersion process, the corrosion solution easily corrodes the surface of the magnesium alloy; therefore, the corrosion resistance of the conversion coating is deteriorated.

Based on the analysis of the above experimental results, it can be seen that the soaking test results are in good agreement with the polarisation and hydrogen evolution curves. From the soaking test, polarisation curve test, and the hydrogen evolution test results, the corrosion resistance of conversion coatings prepared at different temperatures can be arranged in the following increasing order: AZ91D < CO₂_3 MPa_30 min_30 °C < CO₂_3 MPa_80 min_30 °C < CO₂_3 MPa_30 min_40 °C < CO₂_3 MPa_30 min_60 °C < CO₂_3 MPa_30 min_50 °C.

3.3. Reaction Rate

The formation process of magnesium alloy LDH conversion occurs through a series of physical and chemical processes: an electrochemical reaction, ionisation reaction, and coating formation reaction. Several reactions take place at the same time during the initial coating formation. The anodic dissolution reaction occurs, and bubbles appear on the surface of the magnesium alloy, which is caused by the reduction reaction in the micro-cathode area on the surface of the matrix. The initial formation of the LDH conversion coating mainly comprises the precipitation coating of Mg and Al hydroxide, and, at the same time, in the acidic system of CO₂-H₂O (pH = 2.4~3.2), carbonation occurs in the ionisation reaction. Carbonation ionises HCO₃⁻ and CO₃²⁻. With the continuous precipitation of hydrogen from the cathode, the pH value of the substrate surface gradually increases, and insoluble Mg₆Al₂(OH)₁₆CO₃·H₂O is formed. The specific chemical reaction formed by the AZ91D magnesium alloy LDH conversion coating is shown in Equations (4–8)–(4–13) [56–58].



According to the XRD analysis, $\text{Mg}_6\text{Al}_2(\text{OH})_{16}\text{CO}_3 \cdot 4\text{H}_2\text{O}$, the product of Equation (6), is the main component of the coating layer. In Equation (6), the equilibrium constant K of hydroxalite coating is represented as follows:

$$K = \frac{1}{[\text{Mg}^{2+}]^6[\text{Al}^{3+}]^2[\text{CO}_3^{2-}][\text{OH}^-]^{16}} \quad (7)$$

Based on the Arrhenius equation, the reaction rate constant k is a function of temperature T . The reaction in Equation (6) can be considered as a reversible reaction. Therefore,

$$\frac{d \ln k_1}{dT} = \frac{E_a}{RT^2} \quad (8)$$

$$\frac{d \ln k_{-1}}{dT} = \frac{E_{a-1}}{RT^2} \quad (9)$$

In the above formula, k_1 and k_{-1} are the reaction rate constants of the forward and backward reactions in Equation (6). R is the molar gas constant ($\text{KJ} \cdot \text{mol}^{-1}$), T is the absolute temperature, and E_{a1} and E_{a-1} are the activation energies of the forward and backward reactions, which can be obtained from Equations (8) and (9):

$$\frac{d \ln \frac{k_1}{k_{-1}}}{dT} = \frac{E_{a1} - E_{a-1}}{RT^2} \quad (10)$$

Meanwhile, the equilibrium constant K can be expressed as follows:

$$K = \frac{k_1}{k_{-1}} \quad (11)$$

From Equations (10) and (11), it can be deduced that:

$$\frac{d \ln K}{dT} = \frac{E_{a1} - E_{a-1}}{RT} \quad (12)$$

The antiderivative of Equation (10) can be obtained from the corresponding relationship between the equilibrium constant and temperature:

$$\ln K = \ln A - \frac{E_a}{RT} \quad (13)$$

where A is the pre-denoted factor, and E_a is the activation energy.

According to Equation (13), K varies with temperature. The formation process of the LDH conversion coating is an endothermic process, and an increase in temperature increases the value of K , which is conducive to the formation of the LDH conversion coating [59–61]. An increase in temperature can promote the ionisation reaction of carbonic acid, thus increasing the concentration of CO_3^{2-} ions in the solution, promoting the anodic dissolution process on the substrate surface, and speeding up the formation process. In addition, increasing the temperature is also conducive to the thermal movement of the reaction molecules in the forming solution, thus greatly speeding up the formation. However, for the $\text{CO}_2\text{-H}_2\text{O}$ formation system, the formation temperature should be controlled within a certain range. Too low or too high a temperature can affect the quality of the LDH conversion coating.

Under a closed-cycle system, the temperature has an important effect on the deposition process of the LDH conversion coating on the AZ91D magnesium alloy. Firstly, the temperature has an important effect on the microstructure of the conversion coating. When the temperature is below 50°C , the LDH conversion coating on the AZ91D magnesium alloy has not grown completely. There are obvious cracks in the joints of the nuclei growth of the conversion coating. When the temperature is above 50°C , visible cracks are caused

due to internal stress as the coating thickens. Moreover, the crystallization state of LDH conversion coating is the best at 50 °C, and the deconvolution peaks of Mg, Al and O can be obviously seen. Secondly, temperature has an important effect on the corrosion resistance of a conversion coating. Compared to the conversion coating at 50 °C, the electropositive for the potential of the conversion coating at 30 °C, 40 °C, 60 °C and 80 °C is lower, and the corrosion current is larger. In particular, at 30 °C, the self-corrosion potential is 1.40 mV, the corrosion current is $80.22 \mu\text{A}\cdot\text{cm}^{-2}$, the hydrogen evolution rate is relatively high, and the corrosion grade is 3G. According to the data in this experiment, from the perspective of micro-structure and corrosion resistance, the formation temperature of the LDH conversion coating should be controlled at 50 °C.

4. Conclusions

(1) Under a closed-cycle system, the LDH conversion coating on AZ91D magnesium alloy is the densest and most complete when the system temperature is 50 °C. The conversion coating mainly comprises C, O, Mg, and Al, and the main phase is $\text{Mg}_6\text{Al}_2(\text{OH})_{16}\text{CO}_3\cdot 4\text{H}_2\text{O}$, revealing a uniform honeycomb morphology.

(2) Under a closed-cycle system, the corrosion potential is -1.36 V vs. SHE, the corrosion current of the LDH conversion coating is $8.92 \mu\text{A}\cdot\text{cm}^{-2}$, the hydrogen evolution rate is $0.155 \text{ mL}\cdot\text{h}^{-1}\cdot\text{cm}^{-2}$, and the corrosion grade of the immersion test is 7G for the LDH conversion coating at the system temperature of 50 °C.

(3) The equilibrium constant K increases with an increase in temperature, and this increase in temperature is conducive to promoting the formation reaction of the AZ91D magnesium alloy LDH conversion coating upwards. However, there is an optimal temperature value for the forming reaction. Considering the overall quality and the corrosion resistance of the conversion coating, the temperature of the LDH conversion coating should be controlled at around 50 °C.

Author Contributions: Conceived and designed the study: X.Z. and J.W. Performed the experiments: X.Z., Z.Y. and L.M. Contributed reagents/materials/analysis tools: X.Z., B.L., P.Z., Y.Z. and T.Z. Analysed and discussed the data: X.Z., J.W., L.M. and F.W. Wrote the paper: X.Z. Reviewed and edited the manuscript: X.Z., L.M., J.W. and T.Z. Investigation: B.B. All authors have read and agreed to the published version of the manuscript.

Funding: The authors X.C.Z. and Z.J.Y. would like to thank the financial support of the Natural science fund in Heilongjiang projects, the Doctoral Fund of Heilongjiang Institute of Technology, the Provincial Leading Talent Echelon Cultivation Project of Heilongjiang Institute of Technology, the Fundamental Scientific Research Funds for Heilongjiang Provincial Universities, (NO.LH2020E113, 2019BJ14, 2020LJ03, 2020CX05, 2020CX06).

Institutional Review Board Statement: Not applicable.

Informed Consent Statement: Not applicable.

Data Availability Statement: Not applicable.

Conflicts of Interest: The authors declare no conflict of interest.

References

1. Yin, Z.Z.; Qi, W.C.; Zeng, R.C. Advances in coatings on biodegradable magnesium alloys. *J. Magnes. Alloy* **2020**, *8*, 42–65. [[CrossRef](#)]
2. Yang, Y.; Xiong, X.M.; Chen, J. Research advances in magnesium and magnesium alloys worldwide in 2020. *J. Magnes. Alloy* **2021**, *9*, 705–747. [[CrossRef](#)]
3. Panigrahi, S.K.; Mishra, R.S.; Brennan, R.C.; Cho, K. Achieving extraordinary structural efficiency in a wrought magnesium rare earth alloy. *Mater. Res. Lett.* **2020**, *8*, 151–157. [[CrossRef](#)]
4. Pan, H.C.; Xie, D.S.; Li, J.R. Development of novel lightweight and cost-effective Mg–Ce–Al wrought alloy with high strength. *Mater. Res. Lett.* **2021**, *9*, 329–335. [[CrossRef](#)]
5. Li, Z.H.; Sasaki, T.T.; Shiroyama, T. Simultaneous achievement of high thermal conductivity, high strength and formability in Mg–Zn–Ca–Zr sheet alloy. *Mater. Res. Lett.* **2020**, *8*, 335–340. [[CrossRef](#)]

6. Qiu, D.; Zhao, P.; Trinkle, D.R. Stress-dependent dislocation core structures leading to non-schmid behavior. *Mater. Res. Lett.* **2021**, *9*, 134–140. [[CrossRef](#)]
7. Sato, Y.; Swinburne, T.; Ogata, S. Anharmonic effect on the thermally activated migration of $\{101^{-}2\}$ twin interfaces in magnesium. *Mater. Res. Lett.* **2021**, *9*, 231–238. [[CrossRef](#)]
8. Yang, Y.; Chen, X.; Nie, J. Achieving ultra-strong magnesium–lithium alloys by low-strain rotary swaging. *Mater. Res. Lett.* **2021**, *9*, 255–262. [[CrossRef](#)]
9. Kunčická, L.; Kocich, R. Comprehensive characterisation of a newly developed Mg-Dy-Al-Zn-Zr alloy structure. *Metals* **2018**, *2018*, 73. [[CrossRef](#)]
10. Atrens, A.; Song, G.L.; Liu, M. Review of recent developments in the field of magnesium corrosion. *Adv Eng. Mater.* **2015**, *17*, 400–453. [[CrossRef](#)]
11. Xu, J.K.; Cai, Q.Q.; Lian, Z.X. Research progress on corrosion resistance of magnesium alloys with bio-inspired water-repellent properties: A review. *J. Bionic Eng.* **2021**, *18*, 735–763. [[CrossRef](#)]
12. Hu, F.P.; Zhang, Y.; Zeng, Q.W. Research on potassium permanganate-phosphate treatment of magnesium alloy surface and fiber/magnesium alloy composite laminate. *Mater Corros.* **2016**, *67*, 1128–1134. [[CrossRef](#)]
13. Xia, D.H.; Behnamian, Y.; Luo, J.L. Review-factors influencing sulfur induced corrosion on the secondary side in pressurized water reactors (PWRs). *J. Electrochem. Soc.* **2019**, *166*, C49–C64. [[CrossRef](#)]
14. Zhou, M.; Yan, L.C.; Ling, H. Design and fabrication of enhanced corrosion resistance Zn-Al layered double hydroxides films based anion-exchange mechanism on magnesium alloys. *Appl. Surf. Sci.* **2017**, *404*, 246–253. [[CrossRef](#)]
15. Hou, B.R.; Li, X.G.; Ma, X.M. The cost of corrosion in China. *Npj Mater. Degrad.* **2017**, *1*, 4. [[CrossRef](#)]
16. Song, G.L. Recent progress in corrosion and protection of magnesium alloys. *Adv. Eng. Mater.* **2005**, *7*, 563–586. [[CrossRef](#)]
17. Fajardo, S.; Frankel, G.S. A kinetic model explaining the enhanced rates of hydrogen evolution on anodically polarized magnesium in aqueous environments. *Electrochem. Commun.* **2017**, *84*, 36–39. [[CrossRef](#)]
18. Song, G.L.; Amanda, B.L. Corrosion resistance of aged die cast magnesium alloy AZ91D. *Mater. Sci. Eng.* **2004**, *A366*, 74. [[CrossRef](#)]
19. Shao, Z.C.; Cai, Z.Q.; Shi, J.W. Preparation and performance of electroless nickel on AZ91D magnesium alloy. *Mater. Manuf. Processes.* **2016**, *31*, 1238–1245. [[CrossRef](#)]
20. Esmaily, M.; Blücher, D.B.; Svensson, J.E. New insights into the corrosion of magnesium alloys—the role of aluminum. *Scr. Mater.* **2016**, *115*, 91–95. [[CrossRef](#)]
21. Zeng, R.C.; Hu, Y.; Zhang, F. Corrosion resistance of cerium-doped zinc calcium phosphate chemical conversion coatings on AZ31 magnesium alloy. *Trans. Nonferrous Met. Soc.* **2016**, *26*, 472–483. [[CrossRef](#)]
22. Song, G.L.; Shi, Z.M. Corrosion mechanism and evaluation of anodized magnesium alloys. *Corros. Sci.* **2014**, *85*, 126–140. [[CrossRef](#)]
23. Cipriano, A.F.; Lin, J.J.; Miller, C. Anodization of magnesium for biomedical applications—Processing, characterization, degradation and cytocompatibility. *Acta Biomater.* **2017**, *62*, 397–417. [[CrossRef](#)] [[PubMed](#)]
24. Saeki, I.; Seguchi, T.; Kourakat, Y. Ni electroplating on AZ91D Mg alloy using alkaline citric acid bath. *Electrochim. Acta* **2013**, *114*, 827–831. [[CrossRef](#)]
25. Yan, D.L.; Yu, G.; Hu, B.N. An innovative procedure of electroless nickel plating in fluoride-free bath used for AZ91D magnesium alloy. *J. Alloys Compd.* **2015**, *653*, 271–278. [[CrossRef](#)]
26. Wasserbauer, J.; Buchtik, M.; Tkacz, J.; Fintova, S. Improvement of AZ91 alloy corrosion properties by duplex Ni-P coating deposition. *Materials* **2020**, *13*, 61357. [[CrossRef](#)] [[PubMed](#)]
27. Altun, H.K.; Sen, S.D. The effect of PVD coatings on the wear behaviour of magnesium alloys. *Mater. Charact.* **2007**, *58*, 917–921. [[CrossRef](#)]
28. Hoche, H.; Groß, S.; Oechsner, M. Development of new PVD coatings for magnesium alloys with improved corrosion properties. *Surf. Coat. Technol.* **2014**, *259*, 102–108. [[CrossRef](#)]
29. Hurley, M.F.; Efav, C.M.; Davis, P.H. Volta potentials measured by scanning kelvin probe force microscopy as relevant to corrosion of magnesium alloys. *Corrosion* **2015**, *71*, 160–170. [[CrossRef](#)]
30. Williams, G.; Dafydd, H.A.L.; McMurray, H.N. The influence of arsenic alloying on the localised corrosion behaviour of magnesium. *Electrochim. Acta* **2016**, *219*, 401–411. [[CrossRef](#)]
31. Chen, X.B.; Kirkland, N.T.; Krebs, H. In vitro corrosion survey of Mg-xCa and Mg-3Zn-yCa alloys with and without calcium phosphate conversion coatings. *Corros. Eng. Sci. Technol.* **2013**, *47*, 365–373. [[CrossRef](#)]
32. Liu, R.L.; Hurley, M.F.; Kvrryan, A. Controlling the corrosion and cathodic activation of magnesium via microalloying additions of Ge. *Sci. Rep.* **2016**, *6*, 28747. [[CrossRef](#)] [[PubMed](#)]
33. Liu, R.L.; Zeng, Z.R.; Scully, J.R. Simultaneously improving the corrosion resistance and strength of magnesium via low levels of Zn and Ge additions. *Corros. Sci.* **2018**, *140*, 18–29. [[CrossRef](#)]
34. Liu, R.L.; Scully, J.R.; Williams, G. Reducing the corrosion rate of magnesium via microalloying additions of group 14 and 15 elements. *Electrochim. Acta* **2018**, *260*, 184–195. [[CrossRef](#)]
35. Xu, W.; Birbilis, N.; Sha, G. A high-specific-strength and corrosion-resistant magnesium alloy. *Nat. Mater.* **2015**, *14*, 1229–1235. [[CrossRef](#)] [[PubMed](#)]

36. Liu, Q.; Ma, Q.; Chen, G. Enhanced corrosion resistance of AZ91 magnesium alloy through refinement and homogenization of surface microstructure by friction stir processing. *Corros. Sci.* **2018**, *138*, 284–296. [[CrossRef](#)]
37. Carrado, K.A.; Kostapapas, A.; Suib, S.L. Layered double hydroxides (LDHs). *Solid State Ion.* **1988**, *26*, 77–86. [[CrossRef](#)]
38. Wu, L.; Pan, F.S.; Liu, Y.H. Influence of pH on the growth behaviour of Mg-Al LDH films. *Surf. Eng.* **2018**, *34*, 674–681. [[CrossRef](#)]
39. Lin, J.K.; Hsia, C.L.; Uan, J.Y. Characterization of Mg, Al-hydroxalcalite conversion film on Mg alloy and Cl⁻ and CO₃²⁻ anion-exchangeability of the film in a corrosive environment. *Scr. Mater.* **2007**, *56*, 927–930. [[CrossRef](#)]
40. Lin, J.K.; Uan, J.Y. Formation of Mg, Al-hydroxalcalite conversion coating on Mg alloy in aqueous HCO₃⁻/CO₃²⁻ and corresponding protection against corrosion by the coating. *Corros. Sci.* **2009**, *51*, 1181–1188. [[CrossRef](#)]
41. Uan, J.Y.; Lin, J.K.; Sun, Y.S. Surface coatings for improving the corrosion resistance and cell adhesion of AZ91D magnesium alloy through environmentally clean methods. *Thin Solid Films* **2010**, *518*, 7563–7567. [[CrossRef](#)]
42. Uan, J.Y.; Lin, J.K.; Tung, Y.S. Direct growth of oriented Mg-Al layered double hydroxide film on Mg alloy in aqueous HCO₃⁻/CO₃²⁻ solution. *J. Mater. Chem.* **2010**, *20*, 761–766. [[CrossRef](#)]
43. Lin, J.K.; Jeng, K.L.; Uan, J.Y. Crystallization of a chemical conversion layer that forms on AZ91D magnesium alloy in carbonic acid. *Corros. Sci.* **2011**, *53*, 3832–3839. [[CrossRef](#)]
44. Syu, J.H.; Uan, J.Y.; Lin, M.C. Optically transparent Li-Al-CO₃ layered double hydroxide thin films on an AZ31 Mg alloy formed by electrochemical deposition and their corrosion resistance in a dilute chloride environment. *Corros. Sci.* **2013**, *68*, 238–248. [[CrossRef](#)]
45. Yu, B.L.; Lin, J.K.; Uan, J.Y. Applications of carbonic acid solution for developing conversion coating on Mg alloy. *Trans. Nonferrous Met. Soc. China* **2010**, *20*, 1331–1339. [[CrossRef](#)]
46. Chen, J.; Song, Y.W.; Shan, D.Y. In situ growth of Mg-Al hydroxalcalite conversion film on AZ31 magnesium alloy. *Corros. Sci.* **2011**, *53*, 3281–3288. [[CrossRef](#)]
47. Chen, J.; Song, Y.W.; Shan, D.Y. Study of the corrosion mechanism of the in situ grown Mg-Al-CO₃²⁻ hydroxalcalite film on AZ31 alloy. *Corros. Sci.* **2012**, *65*, 268–277. [[CrossRef](#)]
48. Chen, J.; Song, Y.W.; Shan, D.Y. Modifications of the hydroxalcalite film on AZ31 Mg alloy by phytic acid: The effects on morphology, composition and corrosion resistance. *Corros. Sci.* **2013**, *74*, 130–138. [[CrossRef](#)]
49. Chen, J.; Xu, Q.; Song, Y.W. Characterization of the in situ growth manasseite/carbonates composite conversion film on Mg₂Zn alloy. *Mater. Lett.* **2015**, *150*, 65–68. [[CrossRef](#)]
50. Chen, J.; Song, Y.W.; Shan, D.Y. Influence of alloying elements and microstructure on the formation of hydroxalcalite film on Mg alloys. *Corros. Sci.* **2015**, *93*, 90–99. [[CrossRef](#)]
51. Zhang, F.; Liu, Z.G.; Zeng, R.C. Corrosion resistance of Mg-Al-LDH coating on magnesium alloy AZ31. *Surf. Coat. Technol.* **2014**, *258*, 1152–1158. [[CrossRef](#)]
52. Zhang, F.; Zhang, C.L.; Song, L. Corrosion of in-situ grown MgAl-LDH coating on aluminum alloy. *Trans. Nonferrous Met. Soc. China* **2015**, *25*, 3498–3504. [[CrossRef](#)]
53. Zhang, X.C.; Jiang, P.; Zhang, C.Y. Anti-corrosion performance of LDH coating prepared by CO₂ pressurization method. *Intern. J. Corros.* **2018**, *2018*, 9696549. [[CrossRef](#)]
54. Zhang, X.C.; Wang, J.X.; Zhang, C.Y. Formation process of an LDHs coating on magnesium alloy by a CO₂ pressurization method. *Coatings* **2019**, *9*, 10047. [[CrossRef](#)]
55. Zhang, X.C.; Zhong, F.; Li, X.P. The effect of hot extrusion on the microstructure and anti-corrosion performance of LDHs conversion coating on AZ91D magnesium alloy. *J. Alloys Compd.* **2019**, *17*, 756–767. [[CrossRef](#)]
56. Thomas, S.; Medhekar, N.V.; Franke, G.S. Corrosion mechanism and hydrogen evolution on Mg. *Curr. Opin. Solid State Mater. Sci.* **2015**, *19*, 85–94. [[CrossRef](#)]
57. Zhang, T.; Li, Y.; Wang, F.H. Roles of beta phase in the corrosion process of AZ91D magnesium alloy. *Corros. Sci.* **2006**, *48*, 1249–1264. [[CrossRef](#)]
58. Zhou, P.; Yang, L.X.; Hou, Y.J. Grain refinement promotes the formation of phosphate conversion coating on Mg alloy AZ91D with high corrosion resistance and low electrical contact resistance. *Corros. Commun.* **2021**, *1*, 47–57. [[CrossRef](#)]
59. Logan, S.R. The origin and status of the arrhenius equation. *J. Chem. Educ.* **1982**, *59*, 279–281. [[CrossRef](#)]
60. Schwaab, M.; Pinto, J.C. Optimum reference temperature for reparameterization of the arrhenius equation. part 1: Problems involving one kinetic constant. *Chem. Eng. Sci.* **2007**, *62*, 2750–2764. [[CrossRef](#)]
61. Liu, Y.T.; Chen, Y.T.; Wang, M.K. Mechanistic study of arsenate adsorption on lithium/aluminum layered double hydroxide. *Appl. Clay Sci.* **2010**, *48*, 485–491. [[CrossRef](#)]